Temperature-shift-suppression scheme for two-photon two-color rubidium vapor clocks

Tin Nghia Nguyen [1] and Thomas R. Schibli [1,2,*]

[1]*Department of Physics, University of Colorado, Boulder, Colorado 80309-0390, USA*
[2]*JILA, NIST, and the University of Colorado, Boulder, Colorado 80309-0440, USA*

We propose a scheme for interrogating a warm rubidium vapor using two different clock lasers. Performance wise, this approach is distinctly different from the recently proposed two-color two-photon rubidium clocks as our scheme does not trade off the ac Stark suppression against an increased sensitivity to the cell temperature or pressure. Instead, our approach compensates both the ac Stark shift and the temperature and pressure-induced frequency shifts. The proposed scheme also makes use of the modulation transfer technique, which enables a two orders of magnitude increase in the signal-to-noise ratio compared to traditional clocks that rely on fluorescence measurements.

I. INTRODUCTION

Ultrastable optical atomic clocks are crucial for applications involving positioning, navigation, and timing (PNT), and have found their place at the heart of many important scientific experiments. To date, the most stable atomic clocks reach fractional frequency instabilities of the order of 10^{-19} and are typically based on single (or few) ions or on a large number of neutral atoms trapped in an optical lattice. Such clocks typically achieve their stability by probing doubly forbidden optical transitions of very narrow linewidths [1,2]. Both types of clocks are housed inside elaborate vacuum systems and require laser cooling of single ions or atomic ensembles down to near absolute zero temperatures. Because of this, such clocks typically occupy cubic meters of space and require a highly skilled group of people to maintain them.

Optical atomic clocks based on warm atomic (or molecular) vapors, on the other hand, neither require a vacuum system nor laser cooling, and their size is typically best measured in liters, rather than cubic meters. These clocks employ a vapor cell that is either slightly heated or cooled beyond room temperature to maintain a desirable vapor pressure. However, such clocks only deliver fractional instabilities at the order of 10^{-12}–10^{-15} [3–8]. This poor stability is not only due to the much broader linewidths of the clock transition (e.g., a few 100 kHz for the $5S_{1/2} \rightarrow 5D_{5/2}$ rubidium two-photon transition), but also due to ac Stark and pressure-induced shifts. These shifts are mainly driven by intensity fluctuations of the probe laser and temperature variations of the vapor cell. Reaching fractional frequency instabilities beyond 10^{-15} impose technologically unrealistic long-term constraints on the laser power and the cell temperature stabilities.

A new scheme was recently proposed to significantly reduce ac Stark-induced shifts to the $5S_{1/2} \rightarrow 5D_{5/2}$ two-photon transition in rubidium vapor clocks by using two counterpropagating laser beams with one laser at a few GHz blue detuned from the $5S_{1/2} \rightarrow 5P_{3/2}$ transition at 780 nm and the other laser at 776 nm and maintaining a suitable ratio of the laser intensities [9]. This scheme also includes a two orders of magnitude increase in the signal-to-noise ratio (SNR) that could allow a higher fractional stability at short timescales. Unfortunately, as discussed later in this paper, this two-color scheme also adds a first-order contribution from the optical Doppler shift to the clock transition due to unequal laser frequencies. This makes this scheme generally more sensitive to the cell temperature variations, which could limit the long-term performance of the clock for a boost in the short-term stability. Here, we propose to employ the two-color method to cancel the residual Doppler shift against frequency shifts induced by cell temperature variations. Due to the flexibility offered by this two-color method, we can achieve a full cancellation of the first-order residual Doppler shift and the temperature-induced pressure shifts without requiring special gas mixtures. This could lead to a vapor clock that is insensitive to both optical power fluctuations and temperature or pressure fluctuations of the atomic vapor. Overall, this would enable liter-sized optical clocks with a stability of the previous-generation cold atomic clocks.

II. THE TWO-PHOTON RUBIDIUM VAPOR CLOCK

A. One-color scheme

The state-of-the-art rubidium vapor clocks employ the two-photon $5S_{1/2} \rightarrow 5D_{5/2}$ transition as the transition of choice [3,6–8,10]. By absorbing two counterpropagating photons from a single laser at a wavelength of 778.1 nm, the Rb atoms can be excited to the $5D_{5/2}$ state, from where they then decay to the $6P_{3/2}$ state and back to the ground state emitting a blue photon at wavelength of 420 nm as shown in Fig. 1(a). By detecting these blue photons with a photomultiplier tube (PMT), the frequency of the 778-nm laser can be tuned to
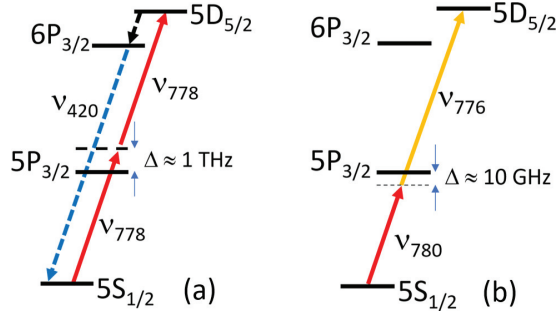
FIG. 1. Energy diagram of the two-photon Rb clock using the $5S_{1/2} \to 5D_{5/2}$ transition following (a) the common single-color scheme with single wavelength of 778.1 nm and (b) the two-color scheme with light at 776- and 780-nm wavelengths for ac Stark shift cancellation and temperature-shift-suppression upgrades.

matched exactly half of the frequency of the $5S_{1/2} \to 5D_{5/2}$ transition. The most common source of 778.1-nm light for these clocks is from the frequency-doubled light of a telecom erbium fiber laser at 1556.2 nm. Due to the maturity of telecom components, these erbium fiber lasers reliably achieve low-intensity noise and ultralow phase noise with laser linewidths narrower than 1 kHz. This ensure a sufficient SNR in such clocks to get the fractional stability at the level of 10^{-13} at 1 s, and 10^{-14} after long averaging times [11]. To improve beyond that, various steps need to be taken to increase the SNR and to minimize or eliminate the sources of shifts in frequency, namely the ac Stark shift, temperature shifts, Zeeman shift, and helium collisional shift. While the Zeeman shift and the helium collisional shift can be mitigated by designing a properly demagnetized multilayer magnetic shield and employing a cell made with aluminosilicate glass, respectively, to achieve 10^{-15} fractional stability, the other two shifts require strict control of the laser power and the temperature of the vapor cell down to the microwatt-level power fluctuation and submillikelvin temperature fluctuation over a 1-day averaging time [7]. These strict requirements make it impractical to maintain the clock stability over long periods of time and would drastically increase the size, weight, and power (SWaP) of such clocks.

B. Two-color scheme

Another clock scheme was proposed by Gerginov and Beloy and by Perrella *et al.* that uses two counterpropagating laser beams at different colors to interrogate the atoms [12], for example: One laser could be a few GHz blue-detuned from the $5S_{1/2} \to 5P_{3/2}$ transition at 780 nm and the other laser is at 776 nm [9]. This scheme features a manyfold increase in SNR due to the smaller detuning of one of the lasers from the $5S_{1/2} \to 5P_{3/2}$ transition (a few GHz compared to 1 THz of the one-color method as shown in Fig. 1), its use of highly efficient silicon photodiodes to detect the laser transmission instead of the PMT, and a larger interaction volume with the atoms. The scheme was also designed to suppress the ac Stark shift by employing the difference in the sign of the polarizability between the 780- and 776-nm excitation pathways, and by maintaining a suitable ratio of the laser intensities. It was found by Gerginov and Beloy that the ac Stark shift can be

completely annihilated if the following condition is satisfied,

$$\frac{I_{780}}{I_{776}} = (0.0656)[1 - (8.06 \times 10^{-3})\Delta - (3.19 \times 10^{-6})\Delta^2], \tag{1}$$

where I_{780} and I_{776} are the intensities of the 780- and 776-nm laser beam, and Δ (in units $2\pi \times$ GHz) is the detuning of the 780-nm laser from the $5S_{1/2} \to 5P_{3/2}$ transition which can take on both positive and negative values, i.e., both blue and red detunings. Unfortunately, a drawback of using two different colors to interrogate the atoms is that the Doppler effect cannot be fully eliminated. This results in a Voigt transition line shape [13], leads to a residual Doppler broadening of the transition line to a couple of MHz at 90 °C [12], and a residual net Doppler shift, which is given by

$$\nu_{780} + \nu_{776} - \nu_{fg} \approx \frac{1}{4\ln 2} \frac{(\nu_{780} - \nu_{776})\nu_{780}(\bar{v}/c)^2}{\nu_{780} - \nu_{ig}}, \tag{2}$$

where ν_{776} and ν_{780} are the frequencies of the 776- and 780-nm lasers, respectively, ν_{fg} is the natural transition frequency between the ground state $5S_{1/2}$ and the excited state $5D_{5/2}$, while ν_{ig} is the transition frequency between the ground state $5S_{1/2}$ and the intermediate state $5P_{3/2}$, $\bar{v} = \sqrt{8k_B T \ln 2/m}$ is proportional to the average speed of the atoms, with k_B being the Boltzmann constant, T being the absolute temperature of the atoms, and m being the mass of a Rb atom for large detunings of the 780-nm laser from the intermediate level. It is clear that the pulling effect is proportional to $\bar{v}^2$ and the temperature T. It should be noted that the sign of the shift depends on the difference between the frequencies of the 780-nm laser and the $5S_{1/2} \to 5P_{3/2}$ transition, and that the pulling effect is strongest for small detunings between these two. The latter two of the remarks can be seen clearly in the region of low detunings in Fig. 2 in the paper presented by Perrella *et al.* [13]. Moreover, by replacing the two wavelengths of 780 nm and 776 nm with a single wavelength at 778 nm in Eq. (2), as for the case of one-color two-photon rubidium clocks, the pulling effect is fully canceled out, as expected.

For the ac Stark shift cancellation method proposed by Gerginov and Beloy, since the 780-nm laser is blue detuned from the $5S_{1/2} \to 5P_{3/2}$ transition, the pulling effect decreases the transition frequency with increasing temperature similar to the Rb-Rb collisional shift and the blackbody radiation shift. A quick calculation of the pulling effect gives a temperature coefficient of -170 Hz/°C for a 10-GHz blue-detuned 780-nm laser, and -860 Hz/°C for a 2-GHz blue-detuned laser at 100 °C cell temperature, respectively. These are of the same order of magnitude as the temperature coefficient of the Rb-Rb collisional shift of -925 to -423 Hz/°C at 100 °C [3,10], and therefore, depending on the choice of the blue detuning of the lasers from the $5P_{3/2}$ state, might not significantly worsen the long-term stability of the clock. However, for small detunings and an effective ac Stark cancellation, this effect might indeed be the residual limit for the long-term stability of the clock. Thus, even though the aforementioned two-color scheme with ac Stark shift cancellation only slightly increases the clock's temperature coefficient, the long-term stability of such clocks might be limited by the temperature stability of the cell.
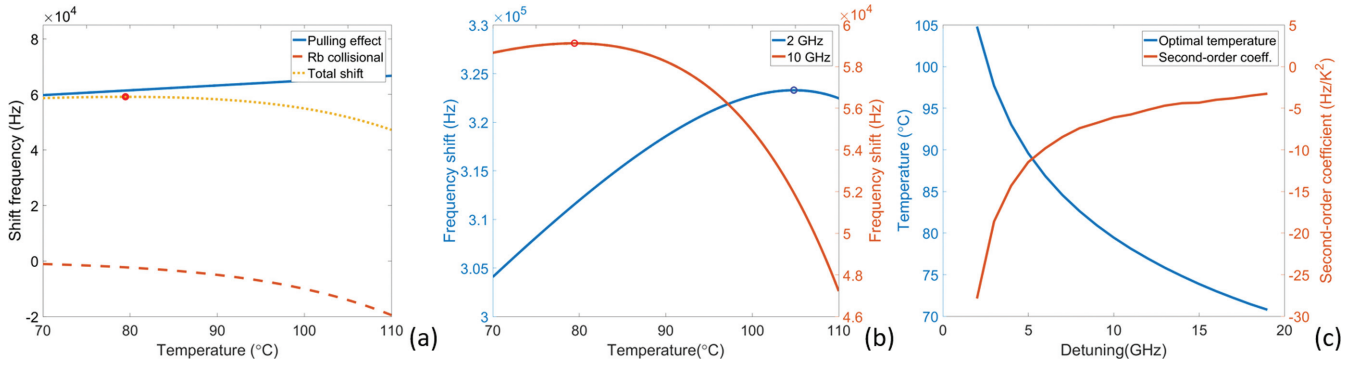
FIG. 2. (a) Contributions of the pulling effect and the collisional shift as a function of the vapor temperature when the 780-nm laser is detuned by 10 GHz below the $5S_{1/2} \rightarrow 5P_{3/2}$ transition. The red circle indicates the location of a local maximum in the total temperature shift. (b) Net-frequency shift as a function of temperature when the 780-nm laser is detuned 2 GHz (blue) and 10 GHz (amber) below the $5S_{1/2} \rightarrow 5P_{3/2}$ transition. The blue and red circles indicate the locations of the local maximum of each curve, where the temperature coefficient vanishes. (c) The optimum temperature and the second-order shift coefficient at the optimum temperature as a function of the detuning of the 780-nm laser.

Now, for the clock scheme by Perrella *et al.*, the 780-nm laser is red detuned by 1.5 GHz from the intermediate state, which could help canceling the Rb-Rb collisional shift. However, since the detuning is relatively small and the pulling effect is inversely proportional to this detuning, the pulling effect outweighs the Rb collisional shift at low temperatures. Simple calculations give the pulling effect shift frequency of 430 kHz at 90 °C, which is much larger than the Rb-Rb collisional shift of −1.82 kHz. The temperature coefficient of the pulling effect can be computed to be 1.2 kHz/°C, which is slightly larger than the temperature coefficient of the Rb-Rb collisional shift mentioned earlier at a comparable temperature. At higher temperatures, the Rb-Rb collisional shift temperature coefficient increases at a faster pace than the pulling effect coefficient due to the exponential increase in Rb vapor pressure. This means that at some temperature higher than 90 °C, the coefficients of these shifts would be the same but opposite, creating a local maximum in the frequency shift plotted against the cell temperature curve. This local maximum would allow a lower temperature-induced frequency shift, and therefore, simpler temperature-stabilizing stabilization methods for the two-color clocks. Hence, we came up with an improved version of the two-color clock scheme to take advantage of this idea.

C. Our scheme

We propose another scheme for the two-photon vapor rubidium clock similar to the methods proposed by Gerginov and Beloy and by Perrella *et al.*, but with a twist. In our proposed method, we make the 780-nm laser red detuned by 10 GHz from the $5S_{1/2} \rightarrow 5P_{3/2}$ transition. This makes the pulling effect take on the sign opposite to the Rb-Rb collisional shift and the blackbody radiation shift, making it a perfect candidate to counter those temperature-induced shifts. The higher detuning compared to the scheme by Perrella *et al.* allows the clock to be operated at a lower optimal temperature for reduced temperature-induced frequency shifts. As shown in Fig. 2(a), the frequency pulling effect can be used to suppress the Rb collisional shift, the main contributor to the total

temperature shift, due to their difference in signs. As a result, we find a local maximum in the temperature-induced shifts. The Rb-Rb collisional shift was calculated from the pressure versus temperature curve of rubidium, while accounting for the approximate factor of two between the measured vapor pressure shift of −27 kHz/mTorr for the $5S_{1/2} \rightarrow 5D_{5/2}$ of ^{85}Rb isotope in a vapor cell with natural Rb compared to the collisional shift in highly enriched ^{87}Rb [7,14]. By operating the vapor cell at a temperature around this local maximum, the dependency of the clock frequency on temperature can be described as $\Delta\nu = a(T - T_{\text{opt}})^2$, where a is the second-order temperature coefficient plotted in Fig. 2(c) for various detunings of the 780-nm laser. For 10 GHz detuning of the 780-nm laser, a takes on a value of −6.12 Hz/K^2, meaning that a temperature drift of as much as 100 mK around the optimal temperature of 79.5 °C would only result in a net frequency change of 0.061 Hz or a contribution to the fractional instability at 8×10^{-17}. This is indeed orders of magnitude smaller compared to what can be achieved by today's one-color clocks' sophisticated temperature stabilizing schemes. A drawback of this scheme is that the optimal temperature depends on the detuning of the 780-nm laser as shown in Fig. 2(b). Therefore, the 780-nm laser frequency needs to be stabilized relative to another laser probing the $5S_{1/2} \rightarrow 5P_{3/2}$ transition, which can be addressed by either sending a second probing laser through the same cell locking it to the $5S_{1/2} \rightarrow 5P_{3/2}$ transition, and locking the beat note between this laser and the 780-nm laser to 10 GHz, or by generating a 10-GHz offset single sideband from the 780-nm probe laser, and locking the sideband to the aforementioned transition.

III. DISCUSSION

The temperature shift suppression scheme closely resembles the clock scheme of Gerginov *et al.*, which not only allows for a manyfold increase in SNR compared to one-color rubidium vapor clocks, but also for the ac Stark shift suppression scheme to be incorporated to result in a scheme that suppresses both the ac Stark shift and the
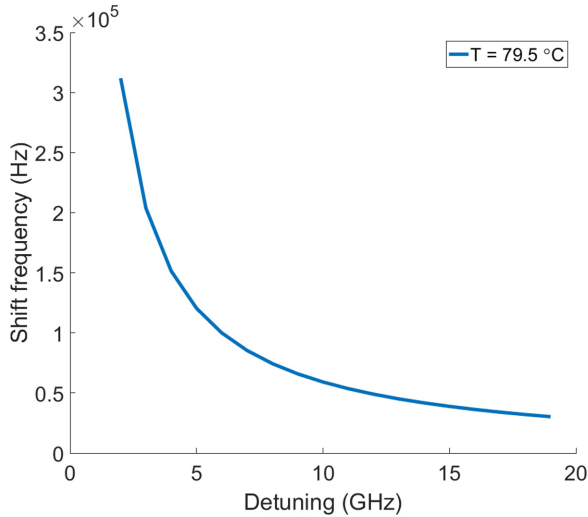
FIG. 3. The shift in transition line as a function of detunings of the 780-nm laser from the $5S_{1/2} \rightarrow 5P_{3/2}$ transition at the optimal temperature for a 10 GHz detuning.

pressure-induced shifts. However, based on Eq. (1), we calculate the ideal intensity ratio of the laser beams, I_{780}/I_{776}, will have to be changed from 0.0602 for a 10-GHz blue-detuned 780-nm laser to 0.0709 for a 10-GHz red-detuned 780-nm laser. For an input power of the 780-nm laser of $P_{780} = 1.2$ mW, a power of $P_{776} = 16.93$ mW is needed to provide the required power ratio of $P_{780}/P_{776} = 0.0709$ for the ac Stark shift cancellation to take effect, given the same beam radius of the two laser beams. Performing a calculation for a 1% power fluctuation in one of the laser diodes around the optimal power values for a beam radius of 1 mm, we found an induced frequency shift of -69.6 Hz or 1.8×10^{-13} fractional instability. Therefore, to achieve a noise floor of, say 3×10^{-15} at 100 s, the absolute power of each laser diode would need to be stabilized to a fractional level of 1.66×10^{-4}. This can be done indeed, as power instabilities at the level of 6×10^{-7} at 100 s was achieved using an acousto-optic modulator for an external cavity diode laser at 7 mW of total output power [15].

An apparent trade-off of this scheme is that the detuning of the 780-nm laser from the $5S_{1/2} \rightarrow 5P_{3/2}$ transition needs to be locked relatively well to 10 GHz as a change in the detuning leads to a frequency shift of the transition line. However, this shift in frequency is drastically reduced with higher detunings of the 780-nm laser, as shown in Fig. 3. For a red detuning of 10 GHz, the change in frequency shift is roughly -12.33 kHz per 1 GHz change of the frequency of the 780-nm laser. This means that to attain a fractional instability of 10^{-15}, the 780-nm laser detuning needs to be stabilized down to the 60 kHz level, which can be done by phase locking the beat note between the 780-nm laser and a laser probing the

$5S_{1/2} \rightarrow 5P_{3/2}$ transition to a low-noise, low-drift oscillator at 10 GHz.

Last but not least, it is important to point out that the arguments and simulations above assumed that the temperature of the atomic vapor and the temperature controlling the vapor pressure to be the same. In reality, the vapor pressure is dictated by the temperature of the coldest spot on the cell wall, usually at the stem of the glass cell, while the temperature of the atomic vapor is given by the cell body temperature. Unfortunately, these temperatures are not the same as observed in a vapor glass cell with long stems [16]. However, these temperatures could be made to be highly or monotonously correlated by having better insulation between the entire glass cell and the environment, and by controlling both temperatures with only one active temperature stabilization loop [16,17]. Then, the temperature set point can be varied to map out the parabolic region of the temperature-induced frequency shift. The existence of the parabolic region is always guaranteed because the temperature coefficient of the frequency pulling effect mostly stays the same while that of the Rb-Rb collisional shift increases with temperature due to the increase in vapor pressure as shown in Fig. 2(a). As a result, the clock can be made to be insensitive to temperature fluctuations by adjusting the set-point temperature to the vertex of the parabolic temperature curve, which might be slightly different from the optimal temperature calculated above.

IV. CONCLUSION

In this paper, we present an analysis of temperature-induced shifts of the proposed two-color clock schemes that could be designed to have a significantly reduced ac Stark shift and a significantly reduced temperature sensitivity. It was found that previous schemes to suppress the instabilities due to the ac Stark shift generally lead to a slightly higher temperature coefficient than that of traditional one-color rubidium vapor clock schemes. This was mainly due to the residual first-order Doppler shift. This effect strongly depends on the chosen blue detuning of the 780-nm laser from the intermediate $5P_{3/2}$ state, and hence might or might not degrade the long-term stability of the clock. Here, we propose another clock scheme to employ this residual Doppler shift to effectively suppress the Rb-Rb collisional shifts at the expense of introducing another laser to probe the $5S_{1/2} \rightarrow 5P_{3/2}$ transition. By phase locking the 780-nm laser to an auxiliary laser probing the $5S_{1/2} \rightarrow 5P_{3/2}$ transition to better than 60 kHz uncertainty, the temperature-induced shift can theoretically be made to be below 10^{-15} fractional instability level. This feature, together with the inherently higher SNR and the ac Stark shift suppression scheme, might enable vapor clocks to attain the frequency stability of the previous-generation table-top cold atomic clocks.

[1] G. E. Marti, R. B. Hutson, A. Goban, S. L. Campbell, N. Poli, and J. Ye, Imaging Optical Frequencies with 100 μHz Precision and 1.1 μm Resolution, Phys. Rev. Lett. **120**, 103201 (2018).

[2] S. M. Brewer, J.-S. Chen, A. M. Hankin, E. R. Clements, C. W. Chou, D. J. Wineland, D. B. Hume, and D. R. Leibrandt, $^{27}Al^+$ Quantum-Logic Clock with a Systematic Uncertainty Below 10^{-18}, Phys. Rev. Lett. **123**, 033201 (2019).

[3] G. Phelps, N. Lemke, C. Erickson, J. Burke, and K. Martin, Compact optical clock with 5×10^{-13} instability at 1 s, J. Inst. Navig. **65**, 49 (2018).

[4] D. Hou, J. Wu, S. Zhang, Q. Ren, Z. Zhang, and J. Zhao, A stable frequency comb directly referenced to rubidium electromagnetically induced transparency and two-photon transitions, Appl. Phys. Lett. **104**, 111104 (2014).

[5] V. Maurice, Z. L. Newman, S. Dickerson, M. Rivers, J. Hsiao, P. Greene, M. Mescher, J. Kitching, M. T. Hummon, and C. Johnson, Miniaturized optical frequency reference for next-generation portable optical clocks, Opt. Express **28**, 24708 (2020).

[6] O. Terra and H. Hussein, An ultra-stable optical frequency standard for telecommunication purposes based upon the $5S_{1/2} \rightarrow 5D_{5/2}$ two-photon transition in rubidium, Appl. Phys. B **122**, 27 (2016).

[7] K. W. Martin, G. Phelps, N. D. Lemke, M. S. Bigelow, B. Stuhl, M. Wojcik, M. Holt, I. Coddington, M. W. Bishop, and J. H. Burke, Compact Optical Atomic Clock Based on a Two-Photon Transition in Rubidium, Phys. Rev. Appl. **9**, 014019 (2018).

[8] L. Hilico, R. Felder, D. Touahri, O. Acef, A. Clairon, and F. Biraben, Metrological features of the rubidium two-photon standards of the BNM-LPTF and Kastler Brossel laboratories, EPJ Appl. Phys. **4**, 219 (1998).

[9] V. Gerginov and K. Beloy, Two-photon Optical Frequency Reference with Active ac Stark Shift Cancellation, Phys. Rev. Appl. **10**, 014031 (2018).

[10] Z. L. Newman, V. Maurice, C. Fredrick, T. Fortier, H. Leopardi, L. Hollberg, S. A. Diddams, J. Kitching, and M. T. Hummon, High-performance, compact optical standard, Opt. Lett. **46**, 4702 (2021).

[11] M. S. Bigelow, K. W. Martin, G. Phelps, and N. D. Lemke, A high performance clock laser for two-photon frequency stabilized optical clocks, in *Conference on Lasers and Electro-Optics*, OSA Technical Digest (online) (Optica Publishing Group, Washington, D.C., 2018), paper JW2A.163.

[12] C. Perrella, P. S. Light, J. D. Anstie, F. N. Baynes, R. T. White, and A. N. Luiten, Dichroic Two-Photon Rubidium Frequency Standard, Phys. Rev. Appl. **12**, 054063 (2019).

[13] C. Perrella, P. S. Light, J. D. Anstie, T. M. Stace, F. Benabid, and A. N. Luiten, High-resolution two-photon spectroscopy of rubidium within a confined geometry, Phys. Rev. A **87**, 013818 (2013).

[14] N. D. Zameroski, G. D. Hager, C. J. Erickson, and J. H. Burke, Pressure broadening and frequency shift of the $5S_{1/2} \rightarrow 5D_{5/2}$ and $5S_{1/2} \rightarrow 7S_{1/2}$ two photon transitions in ^{85}Rb by the noble gases and N_2, J. Phys. B: At. Mol. Opt. Phys. **47**, 225205 (2014).

[15] F. Tricot, D. H. Phung, M. Lours, S. Guérandel, and E. De Clercq, Power stabilization of a diode laser with an acousto-optic modulator, Rev. Sci. Instrum. **89**, 113112 (2018).

[16] C. E. Calosso, A. Godone, F. Levi, and S. Micalizio, Enhanced temperature sensitivity in vapor-cell frequency standards, IEEE Trans. Ultrason. Ferroelectr. Freq. Control **59**, 2646 (2012).

[17] S. Micalizio, C. E. Calosso, A. Godone, and F. Levi, Metrological characterization of the pulsed Rb clock with optical detection, Metrologia **49**, 425 (2012).